International Journal of Computational Intelligence Systems, Vol. 6, No. 4 (July, 2013), 596-608

Support Vector Machine Based Robotic Traversability Prediction with Vision Features

Jianwei Cui[1] , Yan Guo[2] , Huatao Zhang[1] , Kui Qian[1] , Jiatong Bao[3] , Aiguo Song[1] *

[1] *School of Instrument Science and Engineering, Southeast University, Nanjing, 210096, China*

[2] *Electric Power Dispatching and Control Center, Nanjing Electric Power Supply Company, Nanjing, 210019, China*

[3] *School of Energy and Power Engineering, Yangzhou University, Yangzhou, 225009, China*

E-mail: a.g.song@seu.edu.cn

Received 26 October 2010

Accepted 1 January 2013

Abstract

This paper presents a novel method on building relationship between the vision features of the terrain images and the terrain traversability which manifests the difficulty of field robot traveling across one terrain. Vision features of the image are extracted based on color and texture. The travesability is labeled with the relative vibration. The support vector machine regression method is adopted to build up the inner relationship between them. In order to avoid the over-learning during training, *k*-fold method is used and average mean square error is defined as the target minimized to get the optimal parameters based on parameter space grid method. For the traveling smoothness of field robot, the original traversability prediction is transformed to computed traversability prediction based on different initial sub-regions. The optimal path is given by minimizing the sum of computed traversability prediction of all sub-regions in each path. Three experiments are discussed to demonstrate the effectiveness and efficiency of the method mentioned in this paper.

Keywords: support vector machine, traversability prediction, field robot, intelligent decision

1. Introduction

Traversability, which means the difficultly of field robot traveling across one region, is a description of traveling feature for one type of terrain. And traversability prediction is a much more important consideration for the robotics application in the field such as planet exploration, volcano detection, search and rescue work and so on. This prediction plays an unreplaced role in the optimization of path planning for the robots, and consideration of traversability prediction is actually to guide the robots to travel in an unstructured and dangerous terrain environment safely.

In order to evaluate the level of difficulty associated with the traversal of the terrain, Molino develops methods for quantifying the difficulty a robot would encounter traversing such a region of rough terrain. Towards this, three traversability metrics describing rough terrain robot mobility are developed[1].

*Corresponding Author, a.g.song@seu.edu.cn

Seraji introduced the concept of traversability index for the first time which is used for planetary rover [2]. In paper [3], the traversability measure in a fuzzy logic approach has been developed based on terrain qualities including roughness, slope, discontinuity and hardness. Furthermore, several researchers develop the concepts of traversability from other sides. Al-Milli suggests a model with the interaction between the vehicle and the terrain to present the difficulty level of traveling across this terrain and the mode is used in predicting track forces on such terrains [4]. Brooks analyzes the robot's wheel/suspension structure and uses it to distinguish between different terrain the robot is traversing [5]. Ye suggests a traversability field histogram method to transform a local terrain map surrounding the robot's momentary position into a traversability map by extracting the slope and roughness of a terrain patch through least-squares plane fitting[6]. With the developing of embedded computers, it becomes possible to process the vision information real time. Braun adopts a stereo vision based terrain traversability estimation method for off-road mobile robots. The method models surrounding terrain using either sloped planes or a digital elevation model, based on the availability of suitable input data [7]. Howard gives novel techniques for real-time terrain characterization and assessment of terrain traversability for a field mobile robot using a vision system and artificial neural networks. The key terrain traversability characteristics are identified as roughness, slope, discontinuity, and hardness [8]. The group of Kim describes a novel on-line learning method which can make predictions of the traversability properties of complex terrain based on autonomous training data collection which exploits the robot's experience in navigating its environment to train classifiers without human intervention[9] [10]. For the on-line learning method, the training data collected around the robot, and data focus on few types of local terrains and the learning which is lack of information may influence the performance of the robot.

In this paper, the target is to develop the method of building relationship between the vision features of the terrain images and the terrain traversability. An ability of taversability prediction with wide knowledge background is expected, this ability would be used in the path planning and the path optimization. The color and texture features, with which it significantly distinguishes from others, are extracted to form the feature set of one type of terrain, and the relative vibration is used as judgment of traveling difficulty on the terrain. The vision features and relative vibration are received as the input vector and label of SVM regression model which is widely used in self-learning and artificial intelligence application in engineering [11] [12]. Getting the trained SVM regression function, the image of the terrain in front of field robot is linearly divided into several sub-regions where the color and texture features are extracted from. The traversability of every sub-region described with relative vibration will calculated under the SVM regression function using the vision features. We give a novel method for path planning considering the traveling smoothness of field robot, through finding the sub-region with minimal traversability in each row. And the optimization of this path planning depends on minimizing the traversability sum of all the sub-region in each possible path.

The rest of this paper is organized as follows: In section 2, we give a short introduction of SVM regression model. In section 3, we give the description of vision features extraction and relative vibration. And the method of path plan and its optimization are given. Section 4 presents our experiment results, and section 5 concludes the paper and suggests future works.

2. SVM Model

Support vector machine (SVM) belongs to kernel method family. It is also one type of neural learning method. The purpose of developing a SVM model is the identification of the relationship between the selected features input data and result output data. The key idea of SVM is to transfer the nonlinear problem to some high dimensional feature space where could find the approximate linear relationship between inputs and targets, through the first mapping method based on kernel function[13] [14].

2.1. SVM Regression

The intelligent systems for regression estimation can be described as follows.

$$f(\mathbf{x}) = (w \cdot \Phi(\mathbf{x})) + b \tag{1}$$

Given the training sample points with input data vectors and output results $(\mathbf{x_i}, y_i) \in \mathbb{R}^n \times \mathbb{R}, i = 1,2,...,m$, a function $f : \mathbb{R}^n \to \mathbb{R}$ is needed to correctly predict blind examples generated from the same underlying probability distribution as the training sample points. The general SVM regression function take the formula where $w \in \mathbb{R}^n$ is the coefficient matrix, $b \in \mathbb{R}$ and $\Phi(\cdot)$ denotes a non-linear transformation from $\mathbb{R}^n$ to higher dimensional feature space. Our target is to minimize the regression risk with the fixed value of w and b. The optimal regression function is developed with finding the minimum of the followings

$$\begin{aligned} &\min \ \frac{1}{2}\|w\|^2 + C\sum_i^m (\xi_i + \xi_i^*) \\ &suject\ to \quad \begin{cases} y_i - w \cdot \Phi(\mathbf{x_i}) - b \leqslant \varepsilon + \xi_i \\ w \cdot \Phi(\mathbf{x_i}) + b - y_i \leqslant \varepsilon + \xi_i^* \\ \xi_i, \xi_i^* \geqslant 0 \end{cases} \end{aligned} \tag{2}$$

C is balance coefficient and ξ_i,ξ_i^* are the slack variables representing upper and lower constants of the system outputs. And the ε-insensitiveness.

For the numerical computing, the Lagrange function is adopted to build the Lagrange function with saddle point condition

$$\begin{aligned} L(w, \xi_i, \xi_i^*) =& \frac{1}{2}\|w\|^2 + C\sum_i^m (\xi_i + \xi_i^*) \\ &- \sum_{i=1}^m \alpha_i(\varepsilon + \xi_i - y_i + (w \cdot \Phi(\mathbf{x_i})) + b) \\ &- \sum_{i=1}^m \alpha_i^*(\varepsilon + \xi_i^* - y_i - (w \cdot \Phi(\mathbf{x_i})) - b) \\ &- \sum_{i=1}^m (\eta_i \xi_i + \eta_i^* \xi_i^*) \end{aligned} \tag{3}$$

The partial derivative values of w, b, ξ_i, ξ_i^* should equal to zero. Indexed in Eq. 2, the loss function is formulated as follow and the optimization is received through simultaneously minimizing the regression function

$$\begin{aligned} \min \ &\frac{1}{2}\sum_{i,j=1}^m (\alpha_i^* - \alpha_i)(\alpha_j^* - \alpha_j)(\Phi(x_i) \cdot \Phi(x_j)) \\ &+ \sum_{i=1}^m \alpha_i^*(\varepsilon + y_i) + \sum_{i=1}^m \alpha_i(\varepsilon - y_i) \\ &suject\ to \quad \begin{cases} \sum_{i=1}^m (\alpha_i - \alpha_i^*) = 0 \\ \alpha_i, \alpha_i^* \in [0, C] \end{cases} \end{aligned} \tag{4}$$

$(\cdot)$ is the inner product and ε is the value of insensitive coefficient. α_i and α_i^* are the Lagrange multipliers concerned to ξ_i and ξ_i^*. For the convex optimization, we could find that

$$w = \sum_{i=1}^m (\alpha_i - \alpha_i^*)\mathbf{x_i} \tag{5}$$

Depending on the KKT situation, the α_i and α_i^* are equal to 0 which are referred to the sample points in the insensitive area. And the sample points $\mathbf{x_i}$ out of insensitive area, which means that $\alpha_i \neq 0$ and $\alpha_i^* \neq 0$, are the support vectors.

And the final regression function takes the form

$$f(x) = \sum_{i \in SV} (\alpha_i - \alpha_i^*)(\Phi(x_i) \cdot \Phi(x)) + b \tag{6}$$

where SV is the set of support vectors. And the

$$b = \frac{1}{m}\sum_{i=1}^m (y_i - (w \cdot \Phi(\mathbf{x_i})) - \varepsilon) \tag{7}$$

2.2. Kernel Function

Above mentioned $\Phi(\cdot)$, in Eq. 1, denotes a nonlinear transformation from $\mathbb{R}^n$ to higher dimensional feature space. However, the key point $(\Phi(\cdot) \cdot \Phi(\cdot))$ in Eq. 5 is hard to calculate its numerical solution. Fortunately, the kernel function method is adopted to solve this problem: $k(\cdot,\cdot) = (\Phi(\cdot) \cdot \Phi(\cdot))$. So

$$f(x) = \sum_{i \in SV} (\alpha_i - \alpha_i^*)k(x_i, x) + b \tag{8}$$

The kernel function is the type of functions which respect Mercer condition[15]. There are three commonly used kernels and they are
1) Polynomial kernel

$$k(x,y) = (x \cdot y + 1)^p \tag{9}$$

2) Radial basis function

$$k(x,y) = \exp(-\frac{\|x-y\|^2}{2\sigma^2}) \tag{10}$$

3) Sigmoid function

$$k(x,y) = \tanh(v(x \cdot y) + c) \tag{11}$$

2.3. Model Parameters

The performance of the SVM regression depends on the model parameters C and ε, also the parameter of kernel function. Until now, there is no precise method to find the optimal solutions of the values of these parameters. The common method is that building a parameter space with all the alternative parameters of the model and finding the optimization in this space with the target of minimizing the error between the output results in training points and the calculated results of the regression function. And the process of optimization is based on the grid method in the parameter space.

2.4. Training and Testing

Once chosen the model parameters, all the training data should be trained to build up the SVM regression function. In this process, the support vectors would be picked up and the parameters concerned to these support vectors would be fixed. After the training, the regression could give the prediction with the test points that have the same structure with those input vectors in training sample points. And the accuracy of this prediction is defined in terms of mean squared error (MSE) and relative mean squared error (RSE) which are calculated as follows

$$\begin{aligned} MSE &= \frac{1}{m}\sum_{i=1}^{m}(y_i^* - y_i)^2 \\ RSE &= \frac{1}{m}\sum_{i=1}^{m}(\frac{y_i^* - y_i}{y_i})^2 \end{aligned} \tag{12}$$

where m is the number of the test points, y_i is the output result in training point and y_i^* is the prediction result under the regression function.

3. Traversability Prediction Method

Considering the human walking experience, the image of the region in front is captured by eyes and the "features" of this region are extracted and the decision is made based on the relationship, which has been built former, between these "features" and the traveling difficulty of that region. Immigrating this method, we actually hope to find the relationship between the traversability of the ground and vision features extracted from the image of the terrain.

3.1. Vision Features Extraction

The color and texture features are thought significant for the images captured by the onboard camera. The entries of the feature representation are the following:
1) The average value r of the red content in the image.
2) The average value g of the green content in the image.
3) The average value b of the blue content in the image.
4) The mean m of the gray image. The feature is a measurement of average intensity.

$$M = \sum_{i \in H} z_i p(z_i) \tag{13}$$

5) The standard deviation σ of the gray image. The feature is a measurement of average contrast.

$$\sigma = \sqrt{\sum_{i \in H}(z_i - m)^2 p(z_i)} \tag{14}$$

6) The smoothness R of the gray image. The feature is a measurement of the relative smoothness of the intensity in a region , and R is 0 for a region of constant intensity and approaches 1 for regions with large excursions in the values of its intensity levels.

$$R = \frac{\sum_{i \in H}(z_i - m)^2 p(z_i)}{1 + \sum_{i \in H}(z_i - m)^2 p(z_i)} \tag{15}$$

7) The third moment μ_3. The feature is a measurement of the skewness of a histogram. μ_3 is 0 for symmetric histograms, positive by histograms skewed to the right, about the mean, and negative for histograms skewed to the left.

$$\mu_3 = \sum_{i \in H} (z_i - m)^3 p(z_i) \tag{16}$$

8) The uniformity U. The feature is a measurement of uniformity of intensity histogram and is the maximum when all the gray levels are equal.

$$U = \sum_{i \in H} p^2(z_i) \tag{17}$$

9) The entropy e. The feature is a measurement of randomness for the all gray levels of the intensity histogram.

$$e = -\sum_{i \in H} p(z_i) \log_2 p(z_i) \tag{18}$$

In Eq. 13-18, H is the intensity levels, z_i is random variable indicating intensity, and $p(z_i)$ is histogram of the intensity levels. Using these nine features, we create the training and test vector $\mathbf{v}$ of to describe the feature information of each image.

$$\mathbf{v} = \begin{pmatrix} r & g & b & M & \sigma & R & \mu_3 & U & e \end{pmatrix}^T \tag{19}$$

3.2. Traversability Label

For describing the traversability of the terrain where the robot covers, standard deviations of angular accelerations of roll and pitch are adopted. Shown in Fig. 1, φ is the roll and θ is the pitch. So the vibration vector with the meaning of standard deviation of angular acceleration is given as follow

$$\mathbf{L} = \frac{1}{N} \begin{pmatrix} \sqrt{\sum_{i=1}^{N} \left(\ddot{\varphi}_i - \overline{\ddot{\varphi}}\right)^2} & \sqrt{\sum_{i=1}^{N} \left(\ddot{\theta}_i - \overline{\ddot{\theta}}\right)^2} \end{pmatrix} \tag{20}$$

where N is sample number.

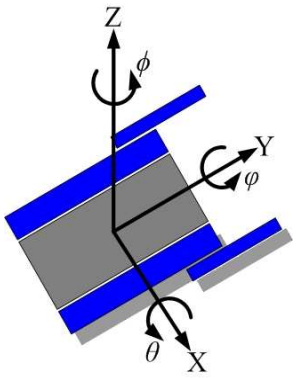

Fig. 1. The coordinate of the robot.

The traversability T represents the difficulty that robot pass through the region. And the relative vibration which is the relative vibration properties in one type of terrain comparing to that on flat ground. It is adopted as traversability label defined in the following form

$$T_i = \frac{\|\mathbf{L}_i\| - \|\mathbf{L}_f\|}{\|\mathbf{L}_i\|} \tag{21}$$

where T_i is the traversability description of ith region, $\mathbf{L}_i$ and $\mathbf{L}_f$ are the vibration vectors in ith region and flat ground. $\|\cdot\|$ is 2-normal function.

3.3. SVM Regression Based Prediction

In order to build up the vision feature training set, the picture of the typical terrain is taken and the training vector in Eq. 19 is extracted as $\mathbf{v}$. And then the field robot should travel cross the ground of this terrain, the Inertia Measurement Unit (IMU) on board would record the roll and pitch angular accelerations data and form the traversability description T under Eq. 21. Repeating this process, we should get the training points $(\mathbf{v}_i, T_i), i = 1, 2, ..., m$. And the SVM regression function could be trained using these points.

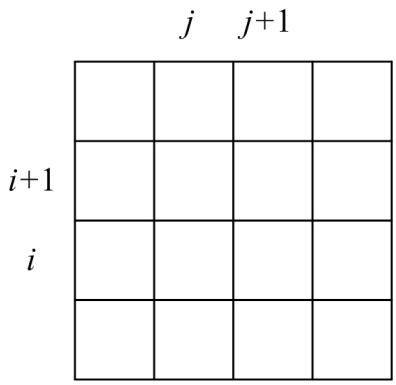

Fig. 2. The sub-regions division.

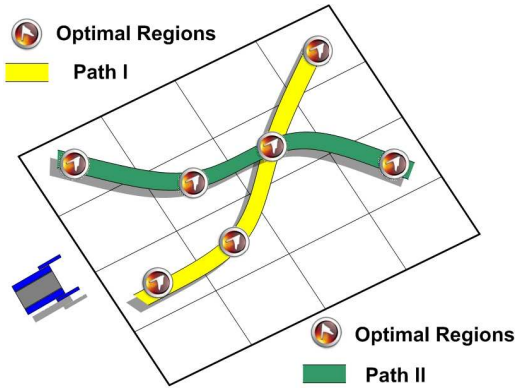

Fig. 3. The pathes from different initial points.

When the field robot runs after the SVM regression function is trained, the camera located on robot would capture the image of the ground in front. The image should be zoomed to suitable processing size and the noise points in image could be filtered with Gauss basis. And then, the image is linearly divided into $K \times K$ sub-regions, shown in Fig. 2. Each sub-region is the testing image unit and the vision features are extracted under Eq. 19 and the traversability prediction of this sub-region is T_i^*.

The general idea about the path planning significantly is a connected line with the optimal sub-regions which have the minimal traversability prediction in each row. But based on original T_i^*, the optimal sub-regions may be discrete in the whole region and that means the path would be a dramatically fluctuating curve which the robot hardly follows with. Considering the traveling smoothness of the field robot, we give a novel method for solving this problem that developing the distance coefficients which values are depending on the distance between the sub-region and the optimal sub-region in the last row. So the optimal sub-region in $(i+1)$th row is

$$\min_j \; S(i+1, j \mid i) \cdot T_{i+1,j}^* \qquad (22)$$

where $\widetilde{T}_{i+1,j} = S(i+1, j \mid i) T_{i+1,j}^*$ is the computed traversability prediction. Because of the distance coefficients added in the system, the optimal sub-regions could be different when we pick different initial sub-regions. In another word, we could find several pathes depending on different initial points, shown in Fig. 3.

Contrasting these pathes, we absolutely hope to find an optimal path with the minimal total traversability and the optimization of path planning is the minimizing the computed traversability prediction sum of all the sub-regions in each path

$$\min_{\tau \in path} \; [\sum_{i=1}^{K} (\min_j S(i+1, j \mid i, \tau) \cdot T_{i+1,j}^*)] \qquad (23)$$

4. Experimental Results

In the previous section, we give a novel method for traversability prediction based on vision features using support vector machine regression. The experiments described in this section are used to demonstrate the effectiveness and performance of this method. The test platform is an field robot ourselves designed with a HD camera and an Crossbow VG400 Inertial Measurement Unit (IMU) [16], shown in Fig. 4, and the SVM implementation in the experiments is referred to the LIBSVM software [17].

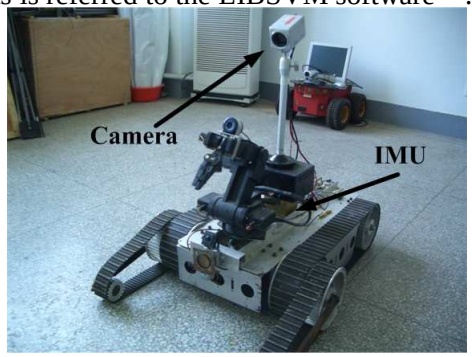

Fig. 4. The field robot used in experiments.

4.1. Data Preparing

The robot shown in Fig. 4 is requested to travel across different terrain shown in Fig. 5.

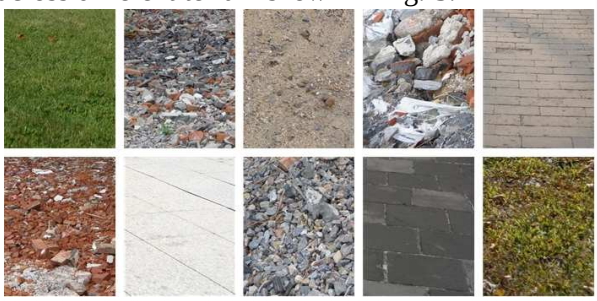

Fig. 5. The part types of training terrain in experiments.

The camera on board takes the pictures of the terrain and the IMU measures the angular acceleration during the traveling. And the vision features are extracted and traversability label are calculated with the above-mentioned methods. Then training points are formed like $(v_i, T_i), i \in 1,2,...300$. And the quantity of the points is 300, parts of the training points are shown in Table 1.

4.2. Parameters Selecting of Model

In practice, an radial basis function (RBF) kernel with reasonable width is good initial trail. In the experiments, the RBF kernel is considered. And the parameters that need to been fixed are σ, ε, C, and the optimal values should be searched in space (σ, ε, C).

Considering ε, the insensitive value of regression function, the less ε means more notice on the error between prediction output of regression function and the traversability label. The continue decreasing of ε will decrease the mean square error with the increasing of support vectors even to all the training points at last and with least MSE. But the model is over-learned that means the new testing points out of training points will hardly get the prediction with the same small level MSE. In another word, the trained regression function has a bad generalization ability.

A k-fold method is used to solve the generalization problem. The train points are divided into k sub-points set which has $300/k$ points. Each set is separately used as testing points and the rest is training points set. $k = 30$ in our experiments. With one parameter point (σ, ε, C), the regression function would be trained 30 times, and there are 30 MSE values of testing points. The average of these MSE value is named AMSE.

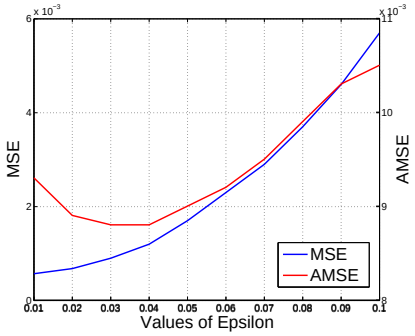

Fig. 6. The values of MSE and AMSE, $\sigma = 0.007, C = 5$.

The curves shown in Fig. 6 present that the MSE decreases when ε decreases, but the AMSE is the lowest at $\varepsilon = 0.03, 0.04$ and it increases back with smaller ε. The AMSE is better than MSE to describe the performance of the parameter point. So the optimization of parameters is to minimize the AMSE in parameter space.

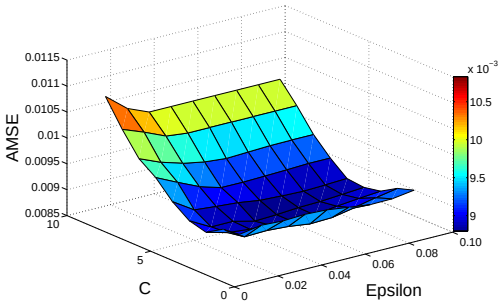

Fig. 7. The values of AMSE based on C, ε, when $\sigma = 0.007$.

Through the approximate calculation, the optimal values of parameters focus on the fields that $\sigma \in [0.001, 0.10]$, $\varepsilon \in [0.01, 0.10]$, $C \in [1, 10]$. The grid method, that calculating the AMSE at each point in parameter space, is used to find the optimal values. The minimal AMSE is at the point $(\sigma, \varepsilon, C) = (0.007, 0.03, 6)$, the final optimal param-

Table 1. Parts of the training points.

No.	*M*	σ	*R*	μ_3	*U*	*e*	*r*	*g*	*b*	*T*
1	75.38	34.02	0.0175	0.5150	0.0093	6.975	91.56	69.69	62.35	0.5188
2	89.78	40.42	0.0245	0.5963	0.0078	7.240	104.70	84.37	77.11	0.5239
3	101.36	33.28	0.0167	0.4243	0.0094	6.988	119.50	94.88	85.80	0.4023
4	104.55	33.71	0.0172	0.3948	0.0091	7.019	121.44	98.72	90.76	0.3944
5	90.22	32.02	0.0156	0.3877	0.0100	6.918	110.45	83.36	72.22	0.4187
6	76.89	30.42	0.0140	0.4784	0.0113	6.787	97.28	69.67	58.53	0.4327
7	64.34	23.33	0.0083	0.1637	0.0135	6.479	83.14	58.55	46.23	0.4904
8	56.33	22.24	0.0075	0.1471	0.0143	6.400	71.19	51.79	41.34	0.5166
9	50.41	22.48	0.0077	0.2091	0.0147	6.361	63.48	45.98	36.33	0.6103
10	51.29	26.50	0.0107	0.1527	0.0112	6.642	58.19	48.48	43.31	0.7515
11	109.91	37.12	0.0208	0.3735	0.0082	7.174	132.05	102.17	92.09	0.5318
12	104.16	38.92	0.0229	0.7644	0.0086	7.163	135.43	93.65	78.58	0.5589
13	110.08	39.74	0.0237	0.8405	0.0086	7.179	140.45	99.43	84.51	0.5470
14	118.42	43.80	0.0287	1.0210	0.0077	7.320	143.57	108.50	96.09	0.5307
15	109.04	37.57	0.0212	0.6631	0.0088	7.121	135.53	99.60	84.39	0.4489
16	141.49	25.02	0.0095	-0.0765	0.0131	6.594	141.10	140.79	142.73	0.4315
17	81.93	30.04	0.0137	0.3595	0.0108	6.812	107.87	73.09	57.98	0.4569
18	76.20	35.52	0.0190	0.9659	0.0102	6.932	97.86	69.84	57.65	0.5880
19	72.30	32.45	0.0159	0.5183	0.0099	6.901	89.19	66.98	56.28	0.5967
20	62.45	28.11	0.0120	0.3810	0.0122	6.660	71.66	59.89	46.81	0.6902
...	...	...	...	...	...	...	...	...	...	....

eters, and the distribution of AMSE at this point is shown in Fig. 7.

4.3. Prediction

With the training points and the optimal parameters mentioned above, the SVM regression function is trained. We take three typical terrain for examples to present the effectiveness. The image in front of robot is divided into 5×5. The coefficient $S(i+1, j \mid i) = 1 + 0.04 \left\| R_{sub}(i+1, j) - R^*_{sub}(i) \right\|$, where R_{sub} is the sub-region in division, R^*_{sub} is that has the minimal traversability prediction in each row and $\|\cdot\|$ is the distance between two sub-regions.

4.3.1. Experiment 1

The first experiment is the terrain with gravel,rock and soil. The prediction difficulty for this terrain is to identify the gravel, rock and soil that have almost the same color but different texture. The image of this terrain is shown in Fig. 8.

Fig. 8. The image of the terrain in the experiment 1.

After vision features extraction, the feature vector is sent to the trained regression function as input. The output of function, which is original traversability prediction is shown in Fig. 9. We could find that this prediction is just based on the nature personalize of terrain without consideration of the traveling smoothness of the field robot.

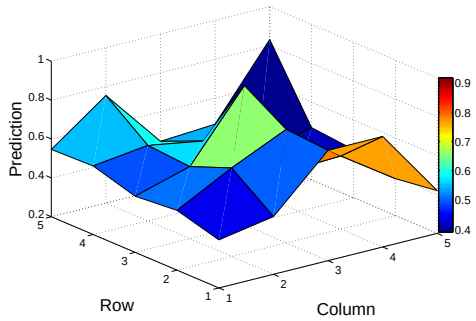

Fig. 9. The original traversability prediction of the experiment 1.

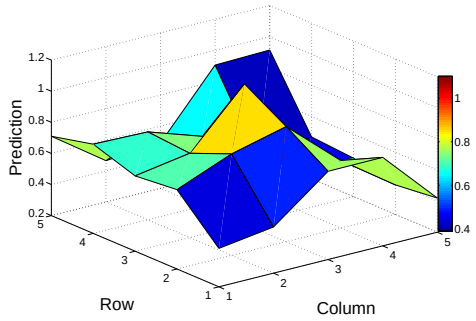

Fig. 10. The $\widetilde{T}$ distribution of optimal path of the experiment 1.

With the method in Eq. 22, we calculate the $\widetilde{T}$ and find the pathes based on different initial subregions. And the optimal path is given under the method in Eq. 23. The $\widetilde{T}$ distribution of the optimal path is shown in Fig. 10.

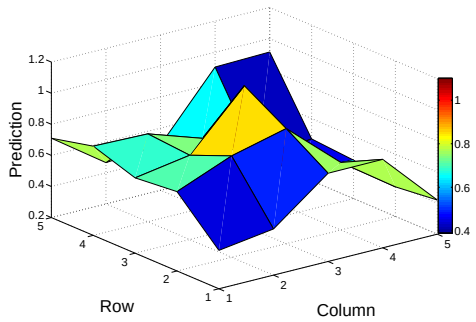

Fig. 11. The $\widetilde{T}$ distribution of optimal path of the experiment 1.

This final traversability prediction is mainly based on the nature personalize: color and texture of the terrain, and partly considered the traveling smoothness of field robot. The optimal path is shown in Fig. 11. This result almost coincides with that is based on our former experience.

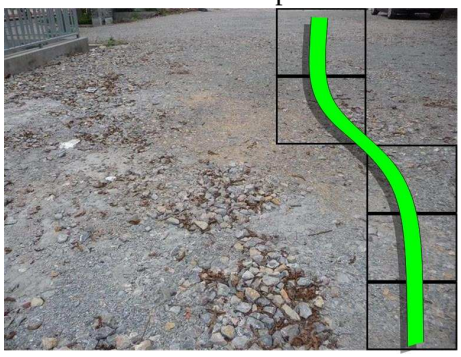

Fig. 12. The final optimal path for the experiment 1.

4.3.2. Experiment 2

Fig. 13. The image of the terrain in the experiment 2.

The terrain as the second experiment is with most of typical obstacles such as stick, gravel,rock, cement block, soil and one piece of grass. The prediction difficulty for this terrain is to identify the items that have complex color feature and texture feature. It is a composite testing of the method given in this paper. The image of this terrain is shown in Fig. 12.

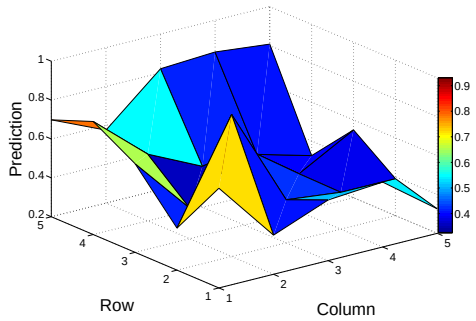

Fig. 14. The original traversability prediction of the experiment 2.

Extracting the vision features and forming the feature vector, the original traversability prediction, through the trained regression function, is given in Fig. 13. This result is also without consideration of traveling smoothness of field robot. We could find that the sub-regions filled with large stick and rock is correctly signed with large traversability prediction values. The method is efficient for this complex terrain.

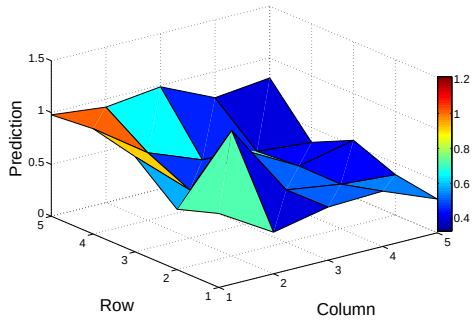

Fig. 15. The $\widetilde{T}$ distribution of optimal path of the experiment 2.

With the methods in Eq. 22 and Eq. 23, we calculate the $\widetilde{T}$ and find the pathes based on different initial sub-regions. And the optimal path is given. The $\widetilde{T}$ distribution of the optimal path is shown in Fig. 14.

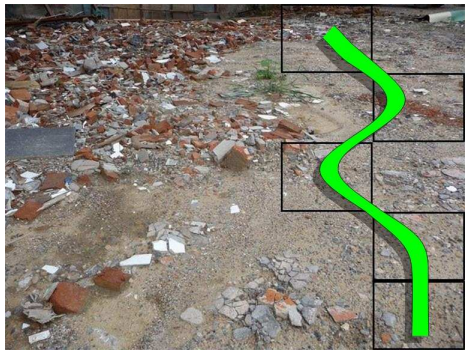

Fig. 16. The final optimal path for the experiment 2.

This final traversability prediction is also mainly considered the nature personalize: color and texture of the terrain, and partly considered the traveling smoothness of field robot. The optimal path is shown in Fig. 15. This result basically coincides with that is based on our former experience.

4.3.3. Experiment 3

Fig. 17. The image of the terrain in the experiment 3.

The third experiment, the terrain full of all various sizes stick, rock and cement block. There is no conspicuous possible optimal path based on observation. The prediction difficulty for this terrain is to give traversability prediction based on seriously familiar color and texture features. It is a special testing hoped to describe the method given in this paper could give the more amazing result than observation with eyes. The image of this terrain is shown in Fig. 16.

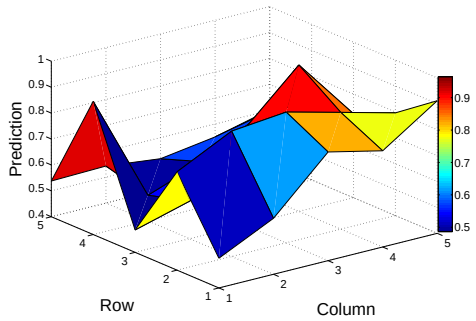

Fig. 18. The original traversability prediction of the experiment 3.

The original traversability prediction under the trained SVM regression function is shown in Fig. 17. We could find that the sub-regions which have little difference on observation could easily separated from each other based on traversability prediction distribution.

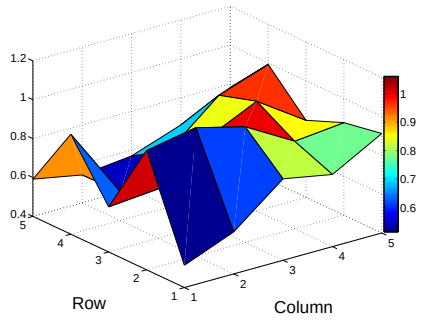

Fig. 19. The $\widetilde{T}$ distribution of optimal path of the experiment 3.

With the methods in Eq. 22 and Eq. 23, we calculate the $\widetilde{T}$ and find the pathes based on different initial sub-regions. And the optimal path is given. The $\widetilde{T}$ distribution of the optimal path is shown in Fig. 18.

Fig. 20. The final optimal path for the experiment 3.

The final optimal path is signed in Fig. 19. This result, suggested by the method mentioned in this paper, presents that the method based on vision features using support vector machine regression could well solve some problems of traversablity prediction of the complex and unstructured terrain that is hardly done with other methods.

4.3.4. Performance

Based on the testing results of above three experiments, the performance is shown in Table 2.

Table 2. The performance of three experiments.

Experiment	1^{st}	2^{nd}	3^{rd}
Height(pixels)	576	576	576
Width(pixels)	768	768	768
$\widetilde{T}$ sum Path 1	2.418	2.693	2.872
$\widetilde{T}$ sum Path 2	2.347	2.423	3.052
$\widetilde{T}$ sum Path 3	2.579	2.497	3.399
$\widetilde{T}$ sum Path 4	2.541	2.423	3.346
$\widetilde{T}$ sum Path 5	2.153	2.254	3.481
Optimal Path	5	5	1
Features Extracted Time(s)	0.49	0.43	0.51
Prediction Time(s)	0.09	0.08	0.06

From the table, the size of the image in each experiment is medium, avoiding the huge computing with large image size and the lack of information with small image size. The $\widetilde{T}$ sums of the pathes with different initial sub-regions are also shown in table. The $\widetilde{T}$ sum of the optimal path has manifest difference from others. The features extracted time and prediction time present the real-time abil-

ity. The sum of two types time is the total time that the method cost during the whole calculating process. The result shows us that this method given in this paper could suggest the traversability prediction with more than 1Hz.

5. Conclusion and Future Works

In this paper, we describe the works on building relationship between the vision features of the ground images and the terrain traversability. Immigrating the thinking of human, we extract the vision features as the personalize description of the terrain based on color and texture features. The travesability, which manifests the difficulty of field robot traveling across one terrain, is labeled with the relative vibration measured with the Inertia Measurement Unit. The support vector machine regression method is adopted to build up the inner relationship between them with the feature vector as input and the traversability label as output. In order to avoid the over-learning during the training of SVM regression function, *k*-fold method is used and average mean square error is defined as the target function minimized. The optimal parameters are given based on parameter space grid method. Considering the traveling smoothness of the field robot, the original traversability prediction is transformed to computed traversability prediction. The pathes with different initial sub-regions is formed and the optimal path is picked up following the minimal sum of computed traversability prediction of all sub-regions in this path. The three experiments are discussed to demonstrate the effectiveness and efficiency of the method mentioned in this paper.

Though this method is useful and efficient for the traversability prediction, the color and texture features are not the only features that could be used in this prediction. We hope to do the research on other type of vision features such as shape, shadow and some abstract features in future. The relative vibration is a good description of traversability, and we also hope to do lots of work to find other description that even better. In future time, another research direction will focus on shorting the feature extracted time and prediction time and increasing the refresh rate of traversability prediction.

Acknowledgements

This research is made possible with support from the Projects under ”Science Innovation Program of Chinese Education Ministry (NO.708045)” and ”National High Technology Research and Development (863 Program) of China (No. 2009AA01Z311)”.

References

1. V. Molino, R. Madhavan, E. Messina, A. Downs, and S. Balakirsky, “A. Jacoff, Traversability metrics for rough terrain applied to repeatable test methods,” *Proc. IEEE International Conference on Intelligent Robots and Systems*, San Diego, USA, 1787–1794 (2007).
2. H. Seraji, “Traversability index:a new concept for planetary rovers,” *Proc. IEEE International Conference on Robotics and Automation*, 2006–2013 (1999).
3. H. Seraji, “A. Howard, Behavior-based robot navagation on challenging terrain: a fuzzy logic approach,” *IEEE Transctions on Robotics and Automation*, **18**, 308–321 (2002).
4. S. Al-Milli and K. Althoefer, “L.D. Seneviratne, Dynamic analysis and traversability prediction of tracked vehicles on soft terrain,” *Proc. IEEE Interantional Conference on Networking Sensing and Control*, London, 279–284 (2007).
5. C. A. Brooks and K. Iagnemma, “Vibration-based terrain classification for planetary expliration rovers,” *IEEE Transctions on Robotics*, **21**, 1185–1191 (2005).
6. G. Ye, “Navigation a mobile robot by a traversability field histogram,” *IEEE Transctions on System,Man,and Cybernetics, Part B: Cybernetics*, **37**, 361–372 (2007).
7. T. Braun, H. Bitsch and K. Berns, “Visual terrain traversability estimation using a combined slope/elevation model,” *Proc. 31st Annual German Conference on Artificial Intelligence*, Kaiserslautern, Germany, 177–184 (2008).
8. A. Howard A and H. Seraji, “Vision-based terrain characterization and traversability assessment,” *Journal of Robotics Systems*, **18**, 577–587 (2001).
9. D. Kim, J. Sun, S. M. Oh, J. M. Regh and A. F. Bobic, “Traversability classification using unsupervised on-line visual learning for outdoor robot navagation,” *Proc. IEEE international Conference on Robotics ans Automation*, ORlando, USA, 518–525 (2006).
10. D. Kim, S. M. Oh and J. M. Rehg, “Traversability classification for UGV navigation,” *Proc. IEEE Inter-*

national Conference on Intenlligent Robots and Systems, San Diego, USA, 3166–3173 (2007).
11. P. Paul, M. Monwar, M. Gavrilova, and P. Wang , "Rotation invariant multiview face detection using skin color regressive model and support vector regression,"*International Journal of Pattern Recognition and Artificial Intelligence*, **8**, 1261–1280 (2010).
12. P. Chen, K. Lee, T. Lee, Y. Lee, and S. Huang, "Multiclass support vector classification via coding and regression," *Neurocomputing*, **7-9**, 1501–1512 (2010).
13. K. Vojislav, "Learning and Soft Computing-Support Vector Machines, Neural Networks, Fuzzy Logic Systems,,, *Cambridge, MA: The MIT Press* (2001).
14. V. N. Vapnik, "An overview of statistical learning theory," *IEEE Transactions on Neural Networks*, **10**, 988–999 (1999).
15. V. N. Vapnik, "Statistical learning theory," *New York: Willey*, (1998).
16. Y. Guo, J. Bao and A. Song, "Designed and implementation of a semi-autonomous search robot," *Proc. IEEE International Conference on Mechatronics and Automation*, Changchun, China, 4621–4626 (2009).
17. C. Chang and C. Lin, "Libsvm: a library for support vector machines," *http://www.csie.ntu.edu.tw/cjlin/libsvm*, (2009)